Available online at www.sciencedirect.com

ScienceDirect

Mendeleev Commun., 2021, **31**, 100–103

Mendeleev Communications

Mechanochemical synthesis of PbS/Ni–Cr layered double hydroxide nanocomposite

Khazangul A. Ibrahimova,*[a] Abdulsaid A. Azizov,[a] Ofeliya O. Balayeva,[a] Rasim M. Alosmanov[a] and Sevinj C. Mammadyarova[b]

[a] *Department of Chemistry, Baku State University, AZ1148 Baku, Azerbaijan. E-mail: khazangul.ibrahimova1994@mail.ru*

[b] *Department of Physics, Baku State University, AZ1148 Baku, Azerbaijan*

DOI: 10.1016/j.mencom.2021.01.031

The synthesis of lead(II) sulfide nanocomposite based on nickel–chromium layered double hydroxide was accomplished by the mechanochemical method at room temperature. The obtained nanocomposites were characterized by powder X-ray diffraction, UV-VIS spectroscopy, scanning electron microscopy and energy-dispersive X-ray spectroscopy to estimate structural, optical and morphological properties. The PbS nanoparticles expanded the interlayer space of the layered double hydroxide, its crystal structure was destroyed, and the PbS nanoparticles attached to the surface affected the XRD result.

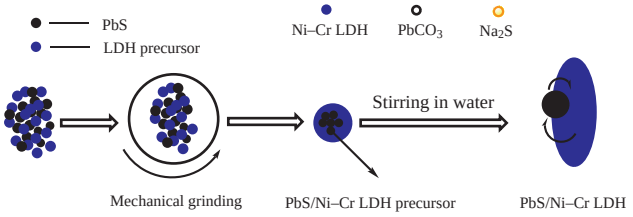

Keywords: layered double hydroxide, lead(II) sulfide nanoparticles, nanocomposite, structural characteristics, optical properties, mechanochemical synthesis.

In recent years, there has been considerable interest in nanoscale chalcogenides due to their remarkable properties and promising application prospects.[1] Semiconductor transition metal sulfides, especially CdS, ZnS and PbS, have been well studied as photocatalysts used in environmental treatment and energy conversion, including degradation of organic matter, hydrogen generation[1] and many other areas such as photoresistive sensors, solar cells, photodetectors and phototransistors.[2]

Among these materials, lead(II) sulfide has attracted much attention for its well-known narrow band gap semiconducting properties.[3] PbS semiconductors have been used in light-emitting diodes, infrared detectors, optical fibers, infrared lasers, window coatings and solar energy panels.[4] This large group of applications is due to its interesting physical properties, such as the Bohr exciton radius (18 nm), small effective masses of electrons and holes, large optical dielectric constant and the infrared direct band gap in the bulk state (0.41 eV at 298 K), which corresponds to the onset of absorption at 3024 nm.[4,5]

One of the promising methods for the synthesis of nanocomposites is based on the use of layered double hydroxides (LDHs) as starting reagents.[6] LDHs are formulated as $(M^{2+})_{1-x}(M^{3+})_x(OH)_2[(A^{n-})_{x/n}\cdot mH_2O]$, where M^{2+} and M^{3+} are metals in the oxidation states of +2 and +3, respectively, and A^{n-} designates almost any anion or anionic complex.[7] More recently, different kinds of LDHs have been widely applied as photocatalysts or photocatalyst carriers due to the advantages of simple preparation, nontoxicity and strong adsorption capacity.[8] This method was used to obtain CdS, PbS, ZnS, Fe, Co, Ni and Cu nanoparticles.[7] Although that the method based on the chemical modification of LDH has many advantages over other methods, its usefulness is limited by the need to select a suitable anionic complex.[10]

In this work, lead(II) sulfide nanocomposite based on nickel–chromium layered double hydroxide (PbS/Ni–Cr LDH) was obtained by the mechanochemical synthesis and characterized by physical methods of analysis.

To prepare nickel–chromium layered double hydroxide (Ni–Cr LDH), we used a one-step co-precipitation method.† Lead(II) sulfide was prepared by the solid-state synthesis‡ using a simple exchange reaction between $PbCO_3$ and Na_2S. With all the necessary starting materials in hand, we synthesized PbS/Ni–Cr LDH nanocomposites by the mechanochemical method§ at room temperature. The obtained nanocomposites were characterized¶ by powder X-ray diffraction (XRD), UV-

† *Synthesis of nickel–chromium layered double hydroxide (Ni–Cr LDH).* Crystal hydrates $NiSO_4\cdot 7H_2O$ (0.015 mol) and $Cr(NO)_3\cdot 9H_2O$ (0.005 mol) were dissolved in distilled water (40 ml) separately, and the resulting two solutions were mixed. The obtained solution was added to a solution of stearic acid (1.9 g) in ethanol (10 ml), titrated with 2 M KOH solution (25 ml) under vigorous stirring and heated at 90 °C for 10 h. The product was washed well with double-distilled water and dried in air.

‡ *Synthesis of lead(II) sulfide.* Lead(II) carbonate (2 g) and sodium sulfide were mixed at a molar ratio of 1 : 1 and mechanically ground in a mortar. After grinding, pure PbS was put into a capped Erlenmeyer flask filled with distilled water (150 ml) and stirred for 2 h using a magnetic stir bar. After that, the solid was washed to completely remove the impurities of sodium ions in the product and dried at room temperature.

§ *Synthesis of PbS/Ni–Cr LDH nanocomposite.* Ni–Cr LDH composite (0.1 g) and dry PbS powder (0.1 g) were mechanically ground in a mortar, mixed with distilled water (25 ml) and stirred for 3 h using a magnetic stir bar. The solid was then washed and dried at room temperature. The synthesis was repeated with ethanol as a solvent.

¶ Powder X-ray diffraction analysis was carried out on a Bruker D2 Phaser diffractometer using CuKα radiation (λ = 0.1541 nm) in the angle

VIS spectroscopy, scanning electron microscopy (SEM) and energy-dispersive X-ray spectroscopy (EDX).

XRD analysis was carried out to investigate the crystalline phase and particle size of the as-prepared product. Figure 1 shows the XRD patterns of Ni–Cr LDH and PbS/Ni–Cr LDH. The presence of highly crystallized products is confirmed by the sharp and symmetric features of the diffraction peaks. The characteristic reflection planes (003), (006), (009), (012) and (110) corresponding to hydrotalcite-like crystal structures (JCPDS file no. 38-0487)[10] were observed at diffraction angles 2θ of 11.86, 23.01, 34.13, 38.76 and 60.34° [Figure 1(*a*)]. The interplanar spacings of LDH are determined by Bragg's law equation[11] from (003) reflection: $d_{(hkl)} = n\lambda/2\sin\theta$, where θ is the scattering angle, n is a positive integer and λ is the wavelength of the incident wave.

The results of XRD analysis confirmed the formation of PbS/Ni–Cr LDH nanocomposites synthesized using water and pure ethanol (Figure 1, curves *2* and *3*, respectively). The characteristic reflection planes (111), (200), (220), (311), (222), (400), (331), (420), (422) and (511), corresponding to the cubic phase of PbS (JCPDS file no. 05-0592)[12] were observed at diffraction angles 2θ of 27.9, 30.17, 43.18, 51.10, 53.82, 62.51, 70.90, 79.14 and 84.98° (Figure 1, curve *3*).

The XRD pattern of PbS/Ni–Cr LDH nanocomposites indicates that they consist of PbS and Ni–Cr LDH, though some diffraction peaks of LDH disappear. We found that the size of PbS nanoparticles is larger than the distance between the layers of LDH. It is because the insertion of PbS expands the interlayer space of LDH, the crystal structure is destroyed, and PbS attached to the surface affects the XRD results. The interplanar spacing of Ni–Cr LDH increased from 7.456 to 16.868 Å, and the XRD pattern of Ni–Cr LDH shows partial changes in the interplanar spacing after PbS attached to the surface affects the LDH (Table 1).

The XRD patterns show that PbS/Ni–Cr LDH nanocomposites obtained from different solutions have a similar crystal structure. LDH materials may include higher water content due to rapid water absorption.[14] Water molecules not only form the hydrate shells of interlayer anions but also are located in various positions of the interlayer space, being attached to the layers by intermolecular hydrogen bonds of various strength.[14–17] The average particle size of the PbS/Ni–Cr LDH nanocomposites

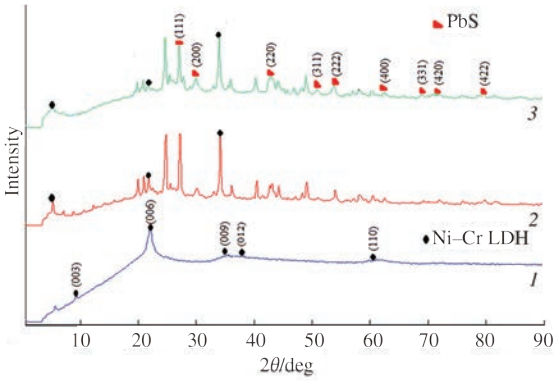

Figure 1 XRD patterns of (*1*) Ni–Cr LDH and nanocomposites (*2*) PbS/Ni–Cr $LDH_{(ethanol)}$ and (*3*) PbS/Ni–Cr $LDH_{(water)}$.

range 2θ = 4–80°. The average size of PbS nanoparticles was calculated using the Debye–Scherrer equation:[9] $D = \alpha\lambda/\beta\cos\theta$, where D is the particle diameter, α is the Scherrer constant equal to 0.9, λ is the X-ray wavelength (1.5418 Å), β is full width at half maximum and θ is the Bragg angle. The UV-VIS absorption spectra were measured on a Specord 210 UV-VIS spectrophotometer. The surface morphology and chemical composition of the products were determined using a JEOL ISM-7600F scanning electron microscope and an X-max 50 energy dispersive X-ray spectrometer, respectively.

Table 1 Structural parameters of Ni–Cr LDH materials determined from the XRD pattern.[a]

Sample	$d_{(003)}$/Å	$d_{(006)}$/Å	$d_{(110)}$/Å	a/Å	c/Å	D/nm
Ni–Cr LDH	7.456	3.862	1.514	3.028	22.368	6.5
PbS/Ni–Cr $LDH_{(ethanol)}$	16.604	4.219	1.584	3.168	49.812	16.8
PbS/Ni–Cr $LDH_{(water)}$	16.868	4.477	1.589	3.178	50.604	24.6

[a] Parameter d is interplanar spacing. Lattice parameters a and c are equivalent to 2 × $d_{(110)}$ and 3 × $d_{(003)}$, respectively. Parameter D is particle diameter.

obtained using ethanol and water as a solvent was determined to be 16.8 and 24.6 nm, respectively. The decrease in the size of particles in pure ethanol can be explained by the influence of organic groups on the stability of the structure. We observed that in combination with LDH, alcohol molecules form stronger hydrogen bonds than water molecules, thereby reducing the distance between the layers. We were able to synthesize PbS/Ni–Cr LDH with a wide interplanar spacing (d_{003} = 16.868 Å) using water as a solvent. Strong and sharp diffraction peaks indicate that the as-prepared products are highly crystalline. As reported, in the course of a mechanochemical reaction, the synthesis of one product influenced the crystallization of other products.[13]

The study of optical properties is of particular importance for the development of new optical devices. Analysis of the optical absorption spectra in a solid material provides important information about the band structure and the energy band gap in materials. We obtained UV-VIS absorption spectra of the samples at 25 °C (Figure 2). The band gap energy was evaluated from the mathematical treatment of the wavelength dependence of optical absorbance data with the following relationship for near-edge absorption. The absorbance generally depends on several factors, such as oxygen deficiency, band gap, impurity centers, grain size, lattice strain and surface roughness.[15] For crystalline semiconductors, their optical band gaps can be calculated from the absorption spectra using the following equation:[16] $\alpha h\nu = A(h\nu - E_g)^{n/2}$, where α, $h\nu$, A and E_g are the absorption coefficient, photon energy, proportionality constant and optical band gap, respectively. The value of n depends on the characteristics of the transition in the semiconductor, more specifically n = 1 for a direct allowed transition and n = 4 for an indirect allowed transition. The value of n = 1 was confirmed here by the published method.[6] The band gap is determined from the intercept of the plot of $(\alpha h\nu)^2$ *vs.* $h\nu$, as shown in Figure 3.

The optical band gaps of Ni–Cr LDH were estimated to be 2.5 and 4.4 eV. The Ni–Cr LDH compound is characterized by higher band gap energy compared to nanocomposites, which is attributed to the presence of organic anions in the LDH galleries. A wider band gap means that more energy is required to excite an electron from the valence band to the conduction band, and

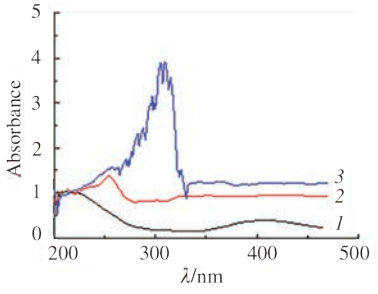

Figure 2 UV-VIS absorption spectra of (*1*) Ni–Cr LDH and nanocomposites (*2*) PbS/Ni–Cr $LDH_{(ethanol)}$ and (*3*) PbS/Ni–Cr $LDH_{(water)}$.

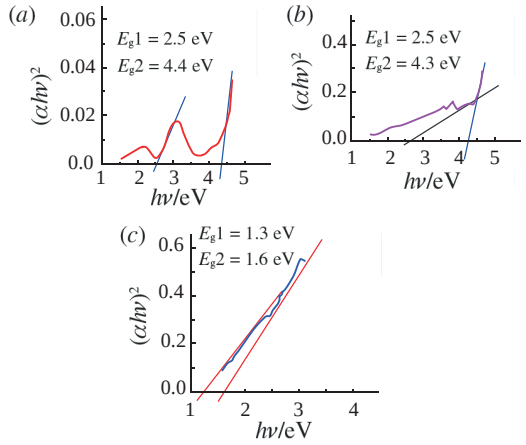

Figure 3 Determination of optical band gaps of (*a*) Ni–-Cr LDH and nanocomposites (*b*) PbS/Ni–-Cr $LDH_{(ethanol)}$ and (*c*) PbS/Ni–Cr $LDH_{(water)}$ from their UV-VIS absorption spectra.

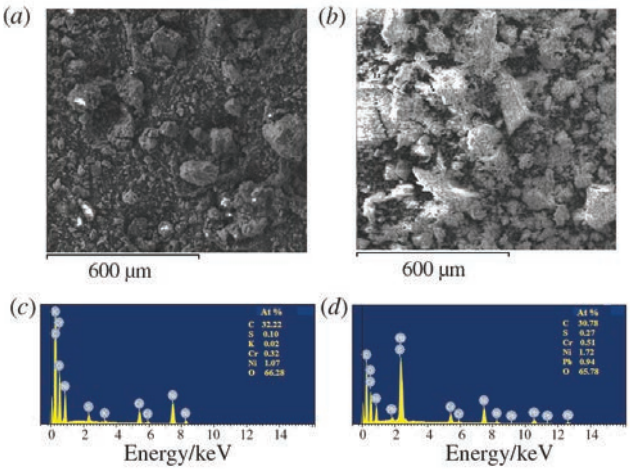

Figure 4 (*a*,*b*) SEM images and (*c*,*d*) EDX spectra of (*a*,*c*) Ni–Cr LDH and (*b*,*d*) PbS/Ni–Cr $LDH_{(water)}$ nanocomposite.

therefore the light with a higher frequency and shorter wavelength will be absorbed.[17] The values of band gap energy and crystallite sizes of samples are given in Table 2. In some structures with degenerate energy levels, if these levels split and became separate, two band gaps are observed, and it is the quantum confinement effect that can split them.[18] The optical band gaps obtained using water and ethanol as a solvent of PbS/Ni–Cr LDH nanocomposites were calculated as 1.3–1.6 and 2.5–4.3 eV, respectively [Figure 3(*b*),(*c*)] , which is higher than the band gap value of PbS in the bulk state (E_g = 0.41 eV at 300 K). This is attributed to the properties of E_g, which depend on crystallite size. The decrease in particle size, which increased the optical band gap energy of the nanoparticles, indicates the presence of the quantum confinement effect, consistent with Brus' theoretical argument.[19,20] The steep absorption edges observed indicate a uniform particle size and morphology with fairly good crystallinity.

The surface morphology of the composites Ni–Cr LDH and PbS/Ni–Cr $LDH_{(water)}$ was characterized by SEM and EDX techniques. Figure 4 shows SEM images of Ni–Cr LDH and PbS/Ni–Cr $LDH_{(water)}$ composites. Hydrotalcite material [Figure 4(*a*)], prepared by the co-precipitation method, has a massive shape and is composed of stacked layered structures. SEM images reveal weakly agglomerated small lumps of irregular shape[21] and large formed particles [see Figure 4 (*a*),(*b*)]. There is no characteristic structure of PbS nanoparticles on the surface, which proves that PbS is distributed over the Ni–Cr LDH surface in the form of dots or a single layer and not agglomerated into spheres [Figure 4(*b*)]. This structure of the composite can provide more active sites, which facilitates the photocatalytic process. During the mechanochemical milling, both growth and breakdown of the particles occurred alternately, thereby preventing excessive particle growth and showing a size of about 10 nm. Since such nanostructured particles were very active, agglomeration occurred, giving the particles a micron-like appearance.

The results of the SEM, EDX and SEM mapping analysis clearly showed the presence of C, O, Cr, Ni, Pb and S in the PbS/Ni–Cr $LDH_{(water)}$ composite with the PbS and LDH phases in the agglomerated particles (Figure 5). And as shown in Figure 4(*d*), the surface of the LDH material has a Pb/S atomic ratio of 3.5. According to the elemental analysis, the concentration of Pb atoms on the surface is maximal. This is due to the different energy states of particles on the surface and in the bulk. The elements must also be redistributed to achieve thermodynamic equilibrium.

In conclusion, we synthesized lead(II) sulfide nanocomposite based on nickel–chromium layered double hydroxide by the mechanochemical method under various reaction conditions. With the clear advantages of facile preparation, stability, low cost and environmental friendliness, this method has a great potential for application in the field of wastewater treatment. An XRD study revealed a nanocrystalline structure with a cubic phase. This is because the insertion of PbS expands the interlayer space of the LDH, the crystal structure is destroyed, and PbS attached to the surface affects the XRD results. The average sizes of PbS nanoparticles were 16.8 and 24.6 nm when using ethanol and water as a solvent, respectively. We managed to synthesize PbS/Ni–Cr LDH with a wide interplanar spacing (d_{003} = 16.868 Å) using water as a solvent. The optical absorption study reveals that PbS nanoparticles have allowed direct transitions. The optical band gap of PbS nanoparticles obtained in water and ethanol was 1.3–1.6 and 2.5–4.3 eV, respectively. The SEM analysis revealed the absence of the characteristic structure of PbS nanoparticles on the surface of the LDH, which proves that PbS is distributed over the Ni–Cr LDH surface in the form of dots or a single layer, and not agglomerated into spheres.

Table 2 The average values of band gap energy and crystallite size of the obtained samples.

Sample	Band gap/eV		Crystallite size/nm
Ni–Cr LDH	2.5	4.4	6.5
PbS/Ni–Cr $LDH_{(ethanol)}$	2.5	4.3	16.8
PbS/Ni–Cr $LDH_{(water)}$	1.3	1.6	24.6

This work was supported by the Department of Polymer Chemistry, Baku State University. The authors thank the Nano Researches Laboratory, BSU, for the XRD results and the Center of Shared Analytical Instruments and Equipment of the Institute of Geology and Geophysics of the Azerbaijan National Academy of Sciences for the SEM results: Nizami M. Sadigov and Mahammedali I. Abdullayev.

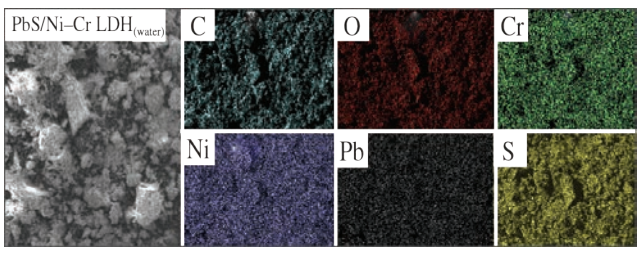

Figure 5 SEM mapping analysis chart of PbS/Ni–Cr $LDH_{(water)}$ nanocomposite.

References

1 L. E. Brus, *Appl. Phys. A: Mater. Sci. Process.*, 1991, **53**, 465.
2 P. Baláž, M. Baláž, E. Dutková, A. Zorkovská, J. Kováč, P. Hronec, J. Kováč, Jr, M. Čaplovičová, J. Mojžiš, G. Mojžišová, A. Eliyas and N. G. Kostova, *Mater. Sci. Eng., C*, 2016, **58**, 1016.
3 N. Soltani, E. Saion, M. Z. Hussein, M. Erfani, A. Abedini, G. Bahmanrokh, M. Navasery and P. Vaziri, *Int. J. Mol. Sci.*, 2012, **13**, 12242.
4 L. Mohapatra, K. Parida and M. Satpathy, *J. Phys. Chem. C*, 2012, **116**, 13063.
5 F. Zhang, N. Du, R. Zhang and W. Hou, *Powder Technol.*, 2012, **228**, 250.
6 P. Mulvaney, L. M. Liz-Marzán, M. Giersig and T. Ung, *J. Mater. Chem.*, 2000, **10**, 1259.
7 P. Scherrer, *Nachr. Ges. Wiss. Goettingen, Math.-Phys. Kl.*, 1918, 98.
8 H. Asiabi, Y. Yamini and M. Shamsayei, *New J. Chem.*, 2018, **42**, 9935.
9 W. H. Bragg and W. L. Bragg, *Proc. R. Soc. London, Ser. A*, 1913, **88**, 428.
10 S. S. Shafiei, M. Solati-Hashjin, H. Rahim-Zadeh and A. Samadikuchaksaraei, *Adv. Appl. Ceram.*, 2013, **112**, 59.
11 K. Kuramoto, S. Intasa-Ard, S. Bureekaew and M. Ogawa, *J. Solid State Chem.*, 2017, **253**, 147.
12 Y. Ao, D. Wang, P. Wang, C. Wang, J. Hou and J. Qian, *Mater. Res. Bull.*, 2016, **80**, 23.
13 G. Prestopino, G. Arrabito, A. Generosi, A. Mattoccia, B. Paci, G. Perez, G. Verona-Rinati and P. G. Medaglia, *Sci. Rep.*, 2019, **9**, 11498.
14 K. Anuar, Z. Zulkarnain, N. Saravanan, A. Zuriyatina and R. Sharin, *Materials Science (Medžiagotyra)*, 2004, **10**, 157.
15 T. Taşköprü, F. Bayansal, B. Şahin and M. Zor, *Philos. Mag.*, 2015, **95**, 32.
16 L. S. Cavalcante, M. A. P. Almeida, W. Avansi, Jr., R. L. Tranquilin, E. Longo, N. C. Batista, V. R. Mastelaro and M. Siu Li, *Inorg. Chem.*, 2012, **51**, 10675.
17 Y. Tian, G. Hua, W. Xu, N. Li, M. Fang and L. Zhang, *J. Alloys Compd.*, 2011, **509**, 724.
18 L. E. Brus, *J. Chem. Phys.*, 1984, **80**, 4403.
19 T. Dippong, F. Goga, E.-A. Levei and O. Cadar, *J. Solid State Chem.*, 2019, **275**, 159.

Received: 17th August 2020; Com. 20/6289